Dalton Transactions

Accepted Manuscript

ROYAL SOCIETY OF CHEMISTRY

www.rsc.org/dalton

Cite this: DOI: 10.1039/c0xx00000x

www.rsc.org/xxxxxx

ARTICLE TYPE

Mixed-ligand ruthenium polypyridyl complexes as apoptosis inducers in cancer cells, the cellular translocation and the important role of ROS-mediated signaling

Zhennan Zhao , Zuandi Luo , Qiong Wu , Wenjie Zheng,* Yanxian Feng, Tianfeng Chen*

Received (in XXX, XXX) Xth XXXXXXXXX 20XX, Accepted Xth XXXXXXXXX 20XX
DOI: 10.1039/b000000x

Ruthenium (Ru) polypyridyl complexes have emerged as leading players among the potential metal-based candidates for cancer treatments. However, the roles of cellular translocation in their action mechanisms remain elusive. Herein we present the synthesis and characterization of a series of ruthenium (Ru) complexes containing phenanthroline derivatives with varying lipophilicities, and examine their mechanism of anticancer action. Results showed that increasing lipophilicity of complexes can enhance the rates of cellular uptake. The *in vitro* anticancer efficacy of these complexes depended on the levels of ROS overproduction, rather than on cellular Ru uptake levels. The introduction of phenolic group on the ligand effectively enhanced the intracellular ROS generation and anticancer activities. Specially, complex **4**, with ortho-phenolic group on the ligand, exhibited better selectivity between cancer and normal cells by comparing with cisplatin. Notably, complex **4** entered the cancer cells partially through transferrin receptor-mediated endocytosis, and then it translocated from lysosomes to mitochondria, where it activated mitochondrial dysfunction by regulation of Bcl-2 family proteins, thus leading to intracellular ROS overproduction. Excess ROS amplified apoptotic signals by activating many downstream pathways such as p53 and MAPKs pathways to promote cell apoptosis. Overall, this study provides a drug design strategy for discovery of Ru-based apoptosis inducers, and elucidates the intracellular translocation of these complexes.

Introduction

The widely use of platinum (Pt)-based drugs is limited by significant toxic side effects, drug resistance and limited selectivity against a broad spectrum of human malignancies.[1] Therefore, it is of great importance to search for substitutes of Pt complexes. Much attention has been paid to ruthenium (Ru), which possesses favorable properties suitable for rational anticancer drug design and biological applications.[2-5] Thus, large number of Ru complexes with different ligands have been synthesized and identified as potential anticancer drugs in the past, and two of them, NAMI-A (*trans*-imidazolium [tetrachloride(dimethylsulfoxide)imidazole ruthenate(III)])[6] and KP 1019 (*trans*-indazolium [tetrachloridobis -(indazole)ruthenate(III)]),[7] have been available as alternatives to Pt complexes for clinical treatment of cancers.[8] Besides NAMI-A-type and KP1019-type complexes, Ru(II) polypyridyl complexes have also been recognized as potent anticancer drug candidates. Due to the unique electrochemical and photophysical properties, Ru polypyridyl complexes have been wide applictions in DNA probing,[9] cellular imaging,[10] protein monitoring,[11] and anticancer cell killing.[12] In the past years, nuclear DNA was known as the target for Ru(II) polypyridyl complexes in cancer cells.[13, 14] However, recent studies show that cytotoxic effects of Ru(II) polypyridyl complexes attributed to other factors, such as mitochondria-mediated apoptosis[15, 16] and topoisomerase I and II inhibition.[17]

Apoptosis is the main mechanism accounting for the anticancer action of metal complexes. These complexes underwent different mode of anticancer actions depending on their accumulation in different cell organelles.[18] Tan et al reported that genomic DNA damage was induced by nuclear permeable Ru complexes, resulting in ROS (reactive oxygen species)-dependent mitochondria dysfunction and finally triggering apoptosis.[19] The lipophilic metal complexes were localized in mitochondria and promoted apoptosis by affecting mitochondrial membrane potential in cells.[20, 21] Lovejoy et al discovered that redox-active Cu complexes were able to induce lysosomal membrane permeability (LMP), which triggered cleavage of Bid and subsequently caused downstream effects on mitochondria.[22] Taking advantages of lipophilic ligands, Cao et al synthesized a series of membrane-localized Ir(III) complexes that induced endoplasmic reticulum (ER) stress and mitochondria-mediated apoptosis in cancer cells.[23] However, there are only a handful of reports which demonstrate the translocation of complexes in different organelles within cells.

Our previous works have found that Ru(II) polypyridyl complexes can inhibit the growth of cancer cell through induction of mitochondria-mediated and DNA damage-mediated p53

phosphorylation, followed by apoptosis.[24, 25] However, the intracellular translocation and the underlying molecular mechanisms accounting for the anticancer action of these Ru complexes remain elusive. For the possibility of complexes location in different cell organelles, real-time monitoring of the cells with florescence microscopy was employed. In order to track the intracellular location of Ru complexes, 2,6-bis(benzimidazol-2-yl) pyridine (bbp) is involved as ancillary ligand, since complexes with bbp derivatives possess properties such as luminescent and good water solubility.[26-28] The mechanism of anticancer action of these complexes was further investigated, which proved more details to biological evaluations of Ru polypyridyl complexes. Results showed that these synthetic complexes entered the cancer cells through transferrin receptor (TfR)-mediated endocytosis, and then they translocated from lysosome to mitochondria, where they activated mitochondrial dysfunction by regulation of Bcl-2 family proteins, thus leading to intracellular ROS overproduction. Excess ROS amplified apoptotic signals by activating many downstream pathways such as p53 and MAPKs pathways to promote cell apoptosis. Notably, increasing lipophilicities of complexes can enhance the rates of cellular uptake but not the anticancer efficacies. We found the anticancer efficacies dependent on the cellular overproduction of ROS level. With phenolic group on the ligand, complex **3** and **4** triggered higher ROS level than complex **1** which exhibited highest cellular accumulation. Among these synthetic complexes, complex **4** exhibited better selectivity between cancer and normal cells by comparison with cisplatin. Overall, this study provides a drug design strategy for discovery of Ru-based apoptosis inducers, and elucidates the intracellular translocation of these complexes.

Results and Discussion

Design, Synthesis and Characterization of Ru(II) Complexes.

The experimental and theoretical results have shown that changes in the positions of phenolic groups on the ligand could cause difference in the properties of Ru(II) polypyridyl complexes.[29] Previous studies found that complexes containing these ligands showed different binding constants (K_b) toward DNA, which motivated us to ascertain the anticancer efficacy caused by structural changes in cancer cells. All the ligands were prepared by a method as previously reported procedure.[26, 30] $Ru(bbp)Cl_3$ was obtained by heating to reflux equal quantity of bbp and $RuCl_3$ in ethanol at 90 ℃ for 3 h. Complexes **1**~**4** (**Scheme 1**) were synthesized by heating to one equivalen of $Ru(bbp)Cl_3$ and corresponding ligand **L** (**L**: pip=2-phenyl-imidazo[4,5-*f*]1,10-phenanthroline, *p*-opip=2-(4-hydroxyphenyl-)imidazo[4,5-*f*]1,10-phenanthroline, *m*-opip=2-(3-hydroxyphenyl-)imidazo[4,5-*f*]1,10-phenanthroline, *o*-opip=2-(2-hydroxyphenyl-)imidazo[4,5-*f*]1,10-phenanthroline) in DMF at 150 ℃ for 5 h, followed by anion exchange with $NaClO_4$ and purification by alumina column chromatography with toluene and methanol as eluant. The synthesized Ru(II) complexes were characterized by ESI mass spectrometry, ^{1}H NMR spectroscopy and elemental analysis (see Experimental Section for further details and Figures S1−S5 in Supporting Information for the mass spectrometry and ^{1}H NMR spectra of Ru complexes). The physicochemical properties of these Ru complexes were also examined. To determine whether all these Ru complexes were stable in physiological environment, we examined the stability of Ru complexes (20 μM) in PBS buffer by UV-Vis spectroscopy. As shown in Figure S6, no obvious change in the UV-Vis absorption spectra of Ru complexes during 24 h-incubation at 25℃ was observed. These results indicated that the intact Ru complexes were responsible for their anticancer activities and biological applications. The lipophilicity of the Ru complexes was examined by determining the distribution coefficients (log*P*) using the "shake-flask" method. As expected, the changes of phenolic group affect the lipophilicity of the Ru complexes. From the data in Table 1, the complex **1** exhibited highest lipophilicity (log*P*=2.26). The lipophilicity of complex **4** was higher than its isomers, which

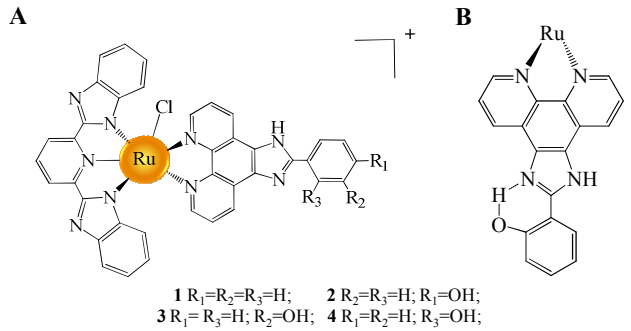

Scheme 1. (A) Structure of Ru complexes in this study. (B) The intermolecular hydrogen bond with *o*-opip ligand**.**

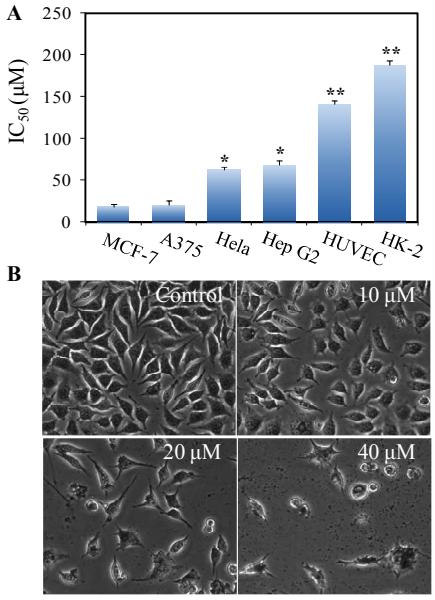

Figure 1. Inhibition of cancer cell proliferation by Ru complexes. (A) IC_{50} values of Ru complex **4** against human cancer and normal cell lines. Significant difference between treatment and control groups is indicated at P <0.05 (*) and P <0.01 (**) levels. (B) Dose-dependent growth inhibition on MCF-7 cells by Ru complex **4**.

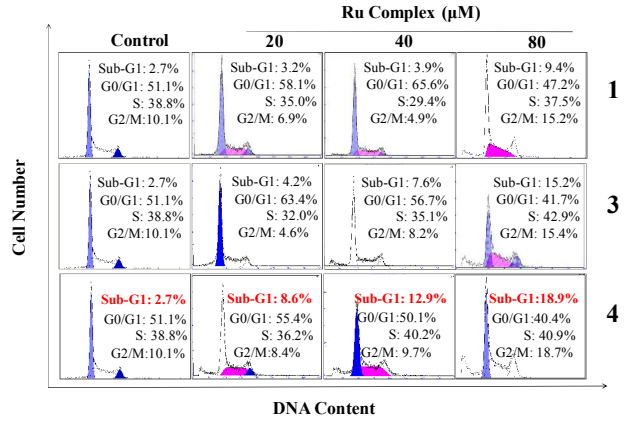

Figure 2. Cell apoptosis inducted by Ru complexes. Apoptotic cell death induced by Ru complexes as examined by propidium iodide (PI)-flow cytometric analysis. Cells were treated with different concentrations of Ru complex **1**, **3** and **4** for 72 h.

may result from the *ortho* phenolic group can form an intermolecular hydrogen bond with the nitrogen atom of the imidazole ring (Scheme 1B). We also found that all these complexes display intense green luminescence in PBS buffer upon irradiation at 381 nm, owing the photophysical properties of bbp ligand (Figure S7). These results showed that the mixed-ligands Ru complexes possessed the physicochemical properties of two individual ligands, which are extremely important to their biological application.

Structure-activity relationship and the induction of cancer cell apoptosis

MTT assay was used to evaluate the effects of the chemical structure of Ru complexes on their cytotoxicities against different human cancer and normal cell lines, including breast adrenocarcinoma MCF-7, hepatocellular carcinoma Hep G2, cervical carcinoma Hela and melanoma A375 cancer lines, umbilical vein endothelial HUVEC and kidney HK-2 cell lines. As shown in Table 1, the synthetic Ru complexes exhibited broad-spectrum inhibition on the growth of human cancer cell lines after a 72-h treatment, by using cisplatin as a positive control. A striking result was that, all the complexes had similar structure, but expressed different antiproliferative activities against different cell lines. The effects of lipophilicity of Ru complexes on cytotoxicity toward cancer cells were entirely different. Complex **2** with para-phenolic group did not present effective inhibition against the tested cell lines. However, complex **3** and **4** with *meta*-phenolic and *ortho*-phenolic group on the ligand showed much higher anticancer efficacy than complex **1** that bears pip ligand. Notably, complex **4** was the most active complex toward all the tested cancer cell lines (Figure 1A). The IC_{50} value of **4** towards MCF-7 cells (Figure 1B) was found at 17.8 μM, which was close to that of cisplatin. Moreover, complex **4** was much less toxic toward human normal cells (Table 1), with IC_{50} values at 187.6 μM (HK-2 kidney cells), which are significantly higher than those of cisplatin 10.3 μM. This rather surprising finding clearly indicated that subtle structural changes have an important impact on the toxicity and prompted us to

Table.1 Cytotoxic effects of Ru complexes on human cancer and normal cell lines

Complex	log*P*	IC_{50}(μM)					
		MCF-7	Hep G2	Hela	A375	HUVEC	HK-2
1	2.26	69.0 ± 3.7	88.9 ± 2.8	156.3 ± 4.8	70.0 ± 3.9	>200	>200
2	0.58	134.2 ± 6.8	129.5 ± 4.2	>200	78.2 ± 5.0	>200	>200
3	1.31	42.7 ± 3.4	76.8 ± 3.8	98.6 ± 2.3	60.3 ± 1.8	>200	>200
4	1.88	17.8 ± 0.8	68.4 ± 1.8	63.2 ± 5.1	30.7 ± 4.1	140.9 ± 9.5	187.6 ± 7.8
Cisplatin	ND	15.7 ± 1.5	13.6 ± 2.0	15.9 ± 1.7	7.3 ± 0.8	ND	10.3 ± 2.1

further investigate the origin of this behavior. Since the MCF-7 cells displayed the most sensitive effort toward all the synthetic complexes, this cell line was selected for further investigation on the underlying mechanisms accounting for the action of Ru complexes. The inhibition of cancer cell proliferation inducted by anticancer drugs could be the result of induction of apoptosis or cell cycle arrest, or a combination of these two modes. From the result of MTT assay, poor antiproliferative activity was observed in complex **2**, and action mechanisms of cell death induced by complexes **1**, **3** and **4** carried out a propidium iodide (PI)-flow cytometric analysis. As shown in Figure 2, exposure of MCF-7 cells to different concentrations of complexes **1**, **3** and **4** for 72 h resulted in different percentage of cells that underwent apoptosis, as reflected by the sub-G1 cell population. The apoptosis-inducing activities of MCF-7 cells were following the order: **4>3>1**, which was consistent with their antiproliferative activities. Moreover, no significant change in cell cycle distribution was observed in cells exposed to complexes, which indicate that cell death induced by Ru complexes are mainly caused by induction of apoptosis.

Uptake and intracellular translocation of the Ru complexes

In order to elucidate the mechanism of action of anticancer activities of Ru complexes, we first study the routes of the cellular entry. As Pucket and Barton reported, endocytosis and active transport proteins are energy dependent while passive diffusion through the membrane and diffusion are not involved with energy.[31] To further dissect the mechanism of the cellular entry of complexes, we assessed whether cellular uptake is energy dependent. In this respect, all these complexes (40 μM) were incubated into MCF-7 cells at 4 and 37 °C for 6 h. As shown in Figure 3A, the cellular uptake of Ru complexes were dependent on their lipophilicities.[23, 32] The uptakes of complexes were significantly increased with temperature, indicating that intracellular uptake involved with energy dependent routes. Furthermore, the intracellular concentrations were fit with the distribution coefficients of Ru complexes at 4 °C, which implied passive diffusion is also contributed to cellular uptake.

To further comfirm the internalization pathway of Ru complexes, cells were pretreated with different endocytosis inhibitors before the addition of Ru complexes (Figure 3B). Treatments of sodium azide (NaN_3) in combination with 2-deoxy-D-glucose (DOG), strongly inhibited the Ru complex internalization to 40.7% of control, which futher proved that Ru complex is transported into the cells by means of energy-dependent pathways. Phagocytosis/macropinocytosis,

caveolae/lipid raft-mediated and clathrinmediated endocytosis are

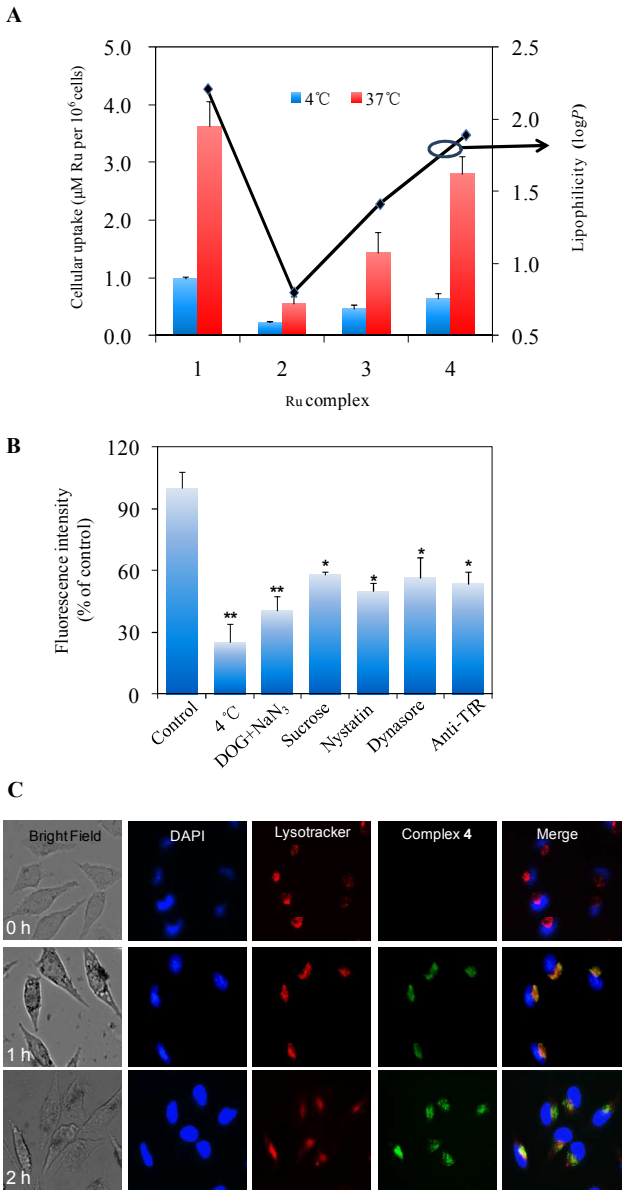

Figure 3. The cellular uptake pathway of Ru complexes. (A) The relationship between cellular uptake and lipophilicity of complexes. Significant difference between treatment and control groups is indicated at P <0.05 (*) and P <0.01 (**) levels. (B) Intracellular uptake of complex **4** in MCF-7 cells under different endocytosis-inhibited conditions. Before the 6 h-incubation of **4** (20 μM), cells were incubated with specific endocytosis inhibitors see Experimental Section for details. The control group was treated with Ru complexes alone for 6 h. Significant difference between treatment and control groups is indicated at P <0.05 (*) and P <0.01 (**) levels. (C) Colocalization of complex **4** and lysosomes in MCF-7 cells. The cells were labeled with Lyso Tracker Red and DAPI, and then exposed to complex **4** (40 μM) for different period of time at 37 ℃.

three main mechanism of endocytosis.[33] Since MCF-7 cells are known to be not phagocytic, the other two pathways were studied. We investigated the cellular uptake of Ru comoplex **4** with continuous treatment of sucrose, a specific inhibitor of clathrin-mediated endocytosis. As we expected, sucrose markedly decreased the internalization of complex **4** to 57.8% of control, indicating that the clathrin-mediated endocytosis was involved. In parallel, nystatin, an inhibitor of lipid raft-dependent endocytosis, caused a reduction to 56.7% of Ru comoplex **4** uptake, demonstrating that lipid raft-mediated endocytosis was also involved in the endocytosis of **4**. Dynamin, a GTP-binding protein, is essential for receptor-mediated endocytosis.[34] Dynasore, a specific inhibitor essential for dynaminmediated lipid raft endocytosis, halted the internalization of complex **4** to 50.2% of control, suggesting that dynamin-mediated pathway was the main pattern of lipid raft-dependent endocytosis of Ru comoplex in MCF-7 cells.

Recent study showed that binding to extracellular serum proteins, such as albumin and transferrin, is likely to promote cellular uptake of Ru(II) complexes through endocytosis.[35] However, handful reports on the interactions between Ru polypyridyl complexes and transferrin have been published.[36] Therefore, we were motivated to investigate the possible role of TfR-mediated endocytosis of Ru complexes. As shown in Figure 3B, the fluorescence intensity of cell group pretreatment with anti-TfR antibody markedly decreased to 53.6% of control compared with the untreated group. This finding reveals that the cellular accumulation of complex **4** is blocked with the decreasing binding site of TfR. For its TfR-mediated endocytosis pathway, we believe that Ru(II) polypyridyl complex exhibited better anticancer activities against MCF-7 cells, which express higher level of TfR on the cell membrane.[37] All the results suggest that Ru(II) polypyridyl complexes were likely to enter cells by a combination of active and passive pathways. Possibly, the increase in lipophilicity of the complexes may affect the cellular uptake by enhancing the passive transport and increasing active transport through hydrophobic interaction with proteins.[38] Taken together, the synthetic Ru complexes exhibit selective cellular uptake in cancer cells through TfR-mediated active transport, but under higher concentrations, this selectivity is lost due to the passive concentration gradient pressure. [39]

Fluorescence imaging technique was also employed to gain more insights into the intracellular trafficking of Ru complex **4**. Form the results of Figure 3C， we found complex **4** can accumulate in a small region of MCF-7 cells, which implied that endocytosis could be a possible way for active transport of Ru complex **4**. Lyso-tracker red was employed for this purpose as it was anticipated that **4** could be localized in the lysosome. Results showed that Ru complex **4** was first accumulated in the lysosomes at 1 h as the great superimposition pattern between the lyso-tracker and **4**. Similar results were observed in the cells treated by Ru complexes **1**~**3** (Figure 4). After another 1h incubation, the observation of intense fluorescence suggests that complex **4** was continually internalized by MCF-7 cells. Moreover, the superimposition pattern between the lyso-tracker and **4** did not match well as previous indicate that complex **4** was capable of escaping from lysosomes and was released into cytosol to activate the downstream signals. These results support our suggestion that the intracellular uptake pathway of Ru

complexes were the combination of endocytosis and passive diffusion. To obtained more insight of the cellular action of complex **4**, the kinetics process of intracellular location of **4** was operated. We anticipated that **4** could be localized in the mitochondria. As shown in Figure 5, a healthy mitochondrial network was extensively interconnected and appeared filamentous, extended throughout the cytoplasm, and the nucleus was in a round shape in control group. After **4** escaped from lysosomes to cytoplasm, we found **4** was accumulated in mitochondria afterwards. Finally,complex **4** diffused throughout the cell at 8 h, and mitochondrial fragmentation, release of mitochondrial contents, nuclear condensation and cytoplasmic shrinkage were observed after 16 h treatment. Similarly, we found complexes **1**, **2** and **3** were also able located in cell mitochondria (Figure 6). These results suggest that mitochondria

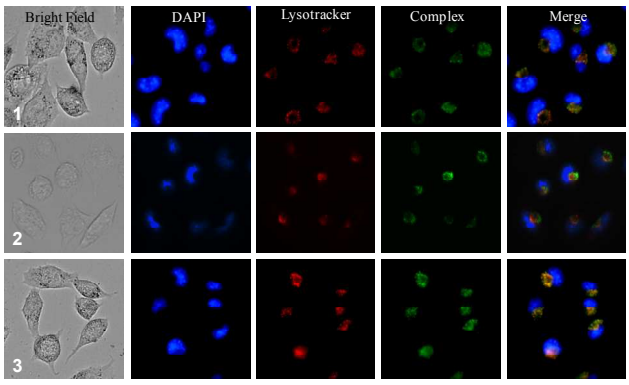

Figure 4. Colocalization of Ru complexes and lysosomes in MCF-7 cells. Cells incubated with Ru complexes **1**~**3** (40 μM) for 1 h.

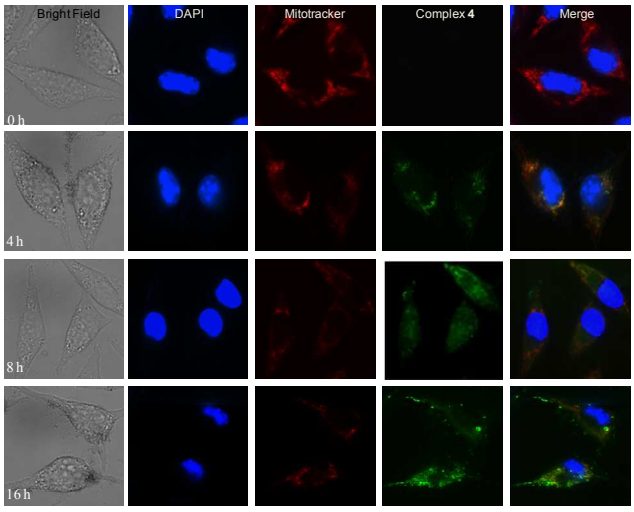

Figure 5. Colocalization of Ru complex and mitochondria in MCF-7 cells. The cells were labeled with Mito Tracker and DAPI, and then exposed to complex **4** (40 μM) for different period of time. Mitochondria, nuclei and Ru complexes were visualized by red, blue and green fluorescence, respectively.

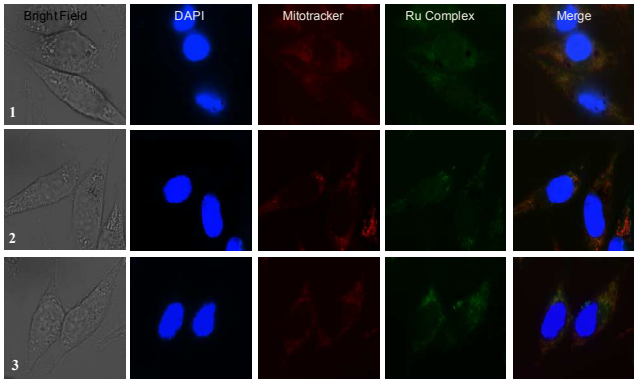

Figure 6. Colocalization of Ru complex and mitochondria in MCF-7 cells. Cells incubated with Ru complexes **1**~**3** (40 μM) for 4 h.

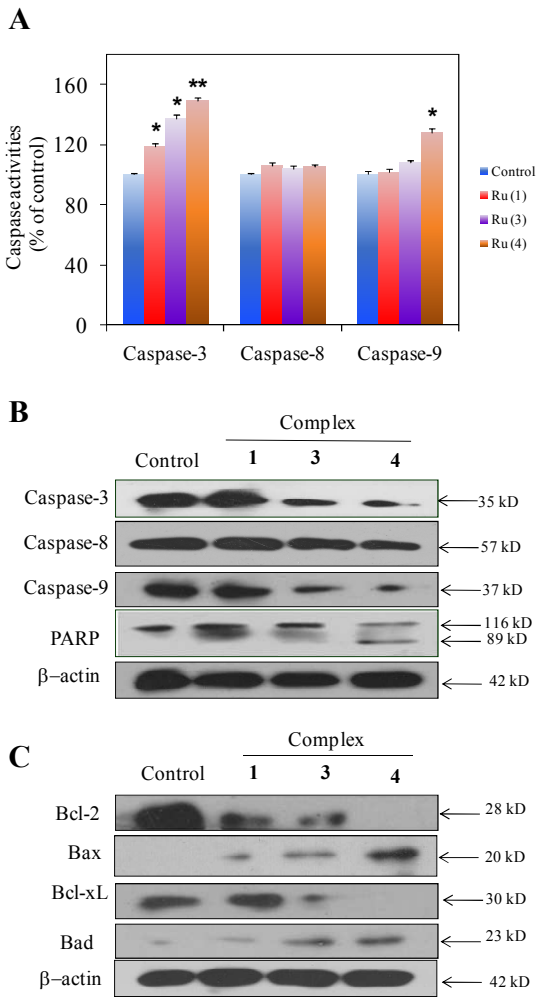

Figure 7. Induction of intrinsic pathway apoptosis by Ru complexes. (A) Caspase activities as measured by specific fluorescent substrates for caspase-3/8/9. Significant difference between treatment and control groups is indicated at P <0.05 (*) and P <0.01 (**) levels. Western blot analysis for (B) the quantitative of caspases activation and PARP cleavage and the expression levels of Bcl-2 family in MCF-7 cells. Equal loading was confirmed by analysis of β-actin in the potein extracts. All result shown here are representative of three independent

experiments with similar results.

Table.2 Absorption spectral and emission spectral properties of Ru complexes bound to G-Quadruplex DNA.

Complex	Absorbance data		Emission data
	H(%)	K_b (10^3M^{-1})	I/I_0
1	13.7	24.3	1.55
2	12.3	6.9	1.47
3	3.8	5.8	1.25
4	10.9	12.5	1.49

* All the experiments were carried out in Tris-HCl/KCl buffer (10 mM Tris-HCl, 100 mM KCl, pH= 7.2). Ru complexes (20 μM) were incubated with increasing concentrations of Bcl-2 G-quadruplex. H is the shortening of hypochromism, K_b is the shortening DNA-binding constant.

could be the destination of Ru complexes in cancer cells.

Ru complexes induced intrinsic apoptosis by triggering mitochondrial dysfunction

Apoptosis can be initiated by two central mechanisms, the extrinsic (death receptor) and intrinsic (mitochondrial) pathways. Caspases,[40] a family of cysteine acid proteases, are known to act as important mediators of apoptosis and contribute to the overall apoptotic morphology by cleavage of various cellular substrates. To delineate the molecular events initiated by Ru complexes, we examined the activities of an executor caspase caspase-3 and two initiator caspases, caspase-8 and caspase-9 by using fluorometric assays. Figure 7A showed that complexes increased the activation of caspase-3/9, while there was no distinct change in the activation of caspase-8. Activation of caspases were further confirmed by cleavage of caspases and PARP as examined by Western blotting. As shown in Figure 7B, treatment with Ru complexes resulted in greatly significantly increased activity of caspase 3/9, which subsequently induced the proteolytic cleavage of PARP, a protein serving as a biochemical mark of cells undergoing apoptosis. These results indicating that intrinsic pathways involved in cells apoptosis and the extrinsic pathways remain inactive.

Mitochondria play a central role in regulation of cell fate by integrating the apoptotic signals originated from both the intrinsic and extrinsic apoptosis pathways. [41] Lipophilic cations are known to accumulate in mitochondria because of the negative potential difference across the mitochondrial membrane [42, 43]. Mitochondria were also considered as target of Ru complexes[15, 16, 21]and our previous work proved that mitochondrial dysfunction led by Ru polypyridyl complexes are critical events in triggering various apoptotic pathways.[24] In this study, the observation of mitochondrial fragmentation and activation of caspase 9 - dependent apoptosis confirms the induction of mitochondrial dysfunction by Ru complexes. Bcl-2 family proteins could regulate outer mitochondrial membrane permeability and control the on/off switching of intrinsic apoptotic pathway. Therefore, we examined the effects of Ru complexes on the expression levels of pro-survival and pro-apoptotic Bcl-2 family proteins in MCF-7 cells by Western blotting. As shown in figure 7C, Ru complexes suppressed the expression level pro-survival Bcl-2 and Bcl-xL protein, but increased the expression levels pro-apoptotic Bcl-2 family proteins Bax and Bad. The down-regulation of Bcl-2/Bax and Bcl-xL/Bad expression ratio suggested that Ru complexes caused the mitochondrial dysfunction in MCF-7 cells. Taken together, these results demonstrate that, inside cancer cells, Ru complexes could translocate from lysosome to mitochondria, where they trigger mitochondrial dysfunction and activation of intrinsic apoptotic pathways.

G-quadruplex DNA is not the principal target of Ru complexes

As mentioned in the introduction, the binding ability of transition metal polypyridyl complexes to nucleic acids was correlated with their cytotoxicity to cancer cells.[44] Studies have demonstrated that G-quadruplex was a rational target for anticancer therapy, since a number of proto-oncogenes have been proved with the G-quadruplex forming potentials in their promoter regions, such as c-myc, c-kit, Bcl-2 and KRAS.[45, 46]A recent work has definitely provided essential evidence for the presence of G-quadruplex structures in the genome of mammalian cells by using engineered antibody.[47] Evidences also proved that G-quadruplex specific ligands regulate the transcription of Bcl-2 through stabilization of quadruplex structure.[48] Ru polypyridyl complexes had reported as G-quadruplex stabilizer[49] with widely applied in anticancer agents[50] and luminescent probes[51]. We therefore investigated the binding of Ru complexes to G-quadruplex Pu 27 (sequence: 5'-CGG GCG CGG GAG GAA GGG GGC GGG AGC-3') within upstream of the Bcl-2 P1 promoter and wonder the down-regulation expression of Bcl-2 in MCF-7 cells could be responsible for interaction between Ru complexes and nucleic acids.

Absorption spectra titrations were performed to determine the binding affinity of complexes to Bcl-2 G-quadruplex. As shown in Table 2 and Figure S8 in the Supporting Information, with increasing amounts of DNA added, the observed hypochromicities follow the order: **1**>**2**>**4**>**3**. The intrinsic binding constants (K_b) follow the order: **1**>**2**>**4**>**3**, which consistent with changes in hypochromicity. To further explore the extent of the interaction of complexes with Bcl-2 G-quadruplex, fluorescence measurements (Figure S9) were performed. Upon excitation using a wavelength of 381 nm for complexes, all of the complexes can emit fluorescence with a maximum wavelength of about 421 nm. A significant 1.55-fold increase in the fluorescence intensity as complex **1** bound to G-quadruplex, while only a slightly fluorescence intensity rose of complex **3**. Taken together, the DNA binding abilities of Ru complexes follow the order: **1**>**4**>**3**, while the suppressed degree of Bcl-2 protein were: **4**>**3**>**1** (Figure 6C). Obviously, these Ru complexes cannot regulate the transcription of Bcl-2 via stabilization of quadruplex structure in living cells. Moreover, from the results of living cell imaging, these Ru complexes inside the cells would translocate from lysosome to mitochondria, without located in the cell nucleus. Therefore, these results suggest that the anticancer action of Ru complexes is independent of their binding affinity of toward G-quadruplex DNA.

ROS-dependent apoptosis induced by mitochondrial dysfunction

The mitochondrial respiratory chain is a potential source of

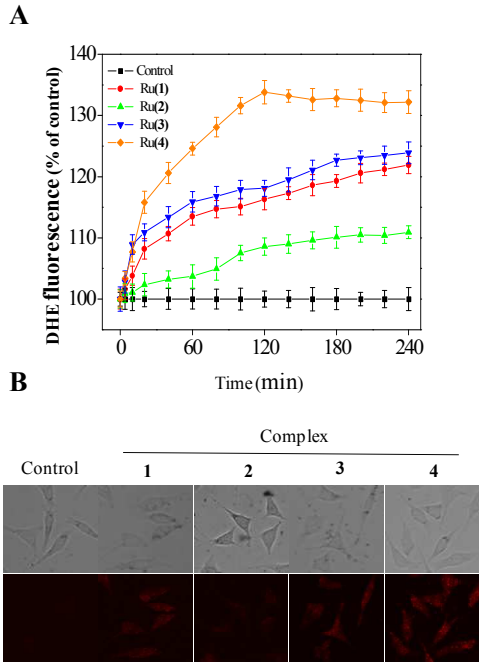

Figure 8. The role of intracellular ROS generation in MCF-7 cell in apoptosis induced by Ru complexes. (A) Effects of concentration on intracellular ROS generation in complexes **1**~**4** (40 μM) treats MCF-7 cells. Cells are treated with 10 mM DHE for 30 min.(B) Fluorescence microscopy images of ROS generation in response to complexes **1**~**4** (40 μM) treatment, as detected by DHE staining.

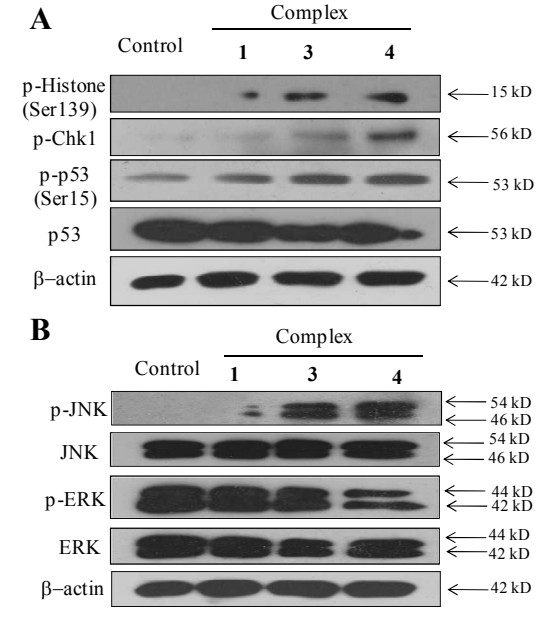

Figure 9. **ROS-mediated signaling pathways triggered by complexes 1, 3 and 4.** Western blot analysis for the expression levels of (A) p-histone, p-Chk1, p-p53, p53 and (B) MAPK signaling pathways in MCF-7 cells. Equal loading was confirmed by analysis of β-actin in the protein extracts. All results shown here are representative of three independent experiments with similar results.

ROS, including superoxide and hydrogen peroxide.[52] ROS has been postulated to play an important role in the induction of apoptosis by various chemopreventive and chemotherapeutic agents.[53, 54] The observation of mitochondrial dysfunction led usto examine the role of ROS in Ru complexes-induced apoptosis. The intracellular ROS generation in MCF-7 cells treated by Ru complexes was measured by dihydroethidium (DHE) fluorescence intensity. Results shown in Figure 8A indicate that complexes **1**~**4** induced ROS generation in MCF-7 cells in a time-dependent manner. Although Ru complexes were able to locate in mitochondria in cancer cells, they activated mitochondrial dysfunction in different degrees. The ROS level triggered by Ru complexes was following this order: **4**>**3**>**1**>**2**, which correlated with their anticancer activities. Despite complex **1** exhibited the highest intracellular accumulation, complex **3** and **4** triggered higher levels of ROS generation. Emission of red fluorescence by the cells after 4 h exposure to Ru(II) complexes (Figure 8B) indicate that these complexes were likely to be localized in the mitochondria. Taken together, these results suggest that excess ROS generation is the main factor contributing to the anticancer efficacy of Ru complexes.

ROS-mediated signaling pathways triggered by Ru(II) complexes.

Studies have shown that ROS could modulate cell apoptosis by regulating diversified downstream signaling pathways.[53] Excess intracellular ROS attacks DNA, resulting in DNA damage and activation of various damage sensor proteins such as ATM and ATR proteins [55, 56]. The signal transmits downstream to checkpoint kinases, such as Chk1 and Chk2, and then to tumor suppressor gene p53. P53 is a major player in the apoptotic response of cells to DNA damage as well as a transcription factor which can directly or indirectly induce cell apoptosis through both the death receptor (extrinsic) and mitochondrial (intrinsic) apoptosis pathways.[57] In this study, we examined the DNA damage marker Histone H2A.X (Ser139) and its downstream kinases Chk1. Western blot analysis shows that Ru complexes treatment causes increased of the expression level of Histone H2A.X (Ser139) and p-Chk1 (Figure 9A). Additionally, we found Ru complexes treatment did not affect the expression level of p53 in cells undergoing apoptosis, but significantly up-regulated the phosphorylation of p53 (ser 15). These results suggest that Ru complexes induce cancer cell p53-activated apoptosis through triggering DNA damage.

MAPKs pathways are primary oxidative stress-sensitive signal transduction pathways in most cell types.[58] To determine the possible role of MAPKs in Ru complexes-induced apoptosis, we checked the status of MAPKs in treated cells (Figure 9B). Among them, JNK was identified as stress-activated protein kinases that activated physical, chemical and biologic stimuli.[59] On the other hand, ERK could prevent cell apoptosis by blocking the cleavage of caspase and control the cell differentiation, proliferation and motility.[60] Herein, we examined the expression level of JNK and ERK of the Ru complexes-treated cells. With the total expression level of kinases remained unchanged, the phosphorylation of antiapoptotic kinases ERK was slightly suppressed by Ru complexes, while the phosphorylation of pro-apoptotic kinases

JNK significantly increased. This result suggests that the up-regulation JNK pathway mainly contributes to apoptosis induced by Ru complexes. Based on the obtained results, the action mechanisms and the underlying signaling pathways of the synthetic Ru complexes were proposed in Figure 10.

Conclusions

Ru polypridyl complexes have emerged as leading players among the potential metal-based candidates for cancer treatments. However, the roles of cellular translocation in their action mechanisms remain elusive. Herein we present the synthesis and characterization of a series of Ru complexes containing phenanthroline derivatives with varying lipophilicities, and examine their mechanism of anticancer action. Results showed that increasing lipophilicities of complexes can enhance the rates of cellular uptake. The *in vitro* anticancer efficacy of these complexes depended on the levels of ROS overproduction. The introduction of phenolic group on the ligand effectively enhanced the intracellular ROS generation and anticancer activities. Specially, complex **4** with *ortho*-phenolic group on the ligand possess optimal lipophilicity among these complexes thus exhibited higher selectivity between cancer and normal cells by comparing with cisplatin. The complex entered cancer cells through TfR-mediated endocytosis, and then it translocated from lysosome to mitochondria, where it activated mitochondrial dysfunction by regulation of Bcl-2 family proteins, thus leading to intracellular ROS overproduction. Excess ROS amplified apoptotic signals by activating many downstream pathways such as p53 and MAPKs pathways to promote cell apoptosis. We suggest that this kind of complexes triggered mitochondria-mediated apoptosis pathway, but not the traditional DNA-binding action mechanisms. Overall, this study provides a drug design strategy for discovery of Ru-based apoptosis inducers, and elucidates the intracellular translocation of these complexes.

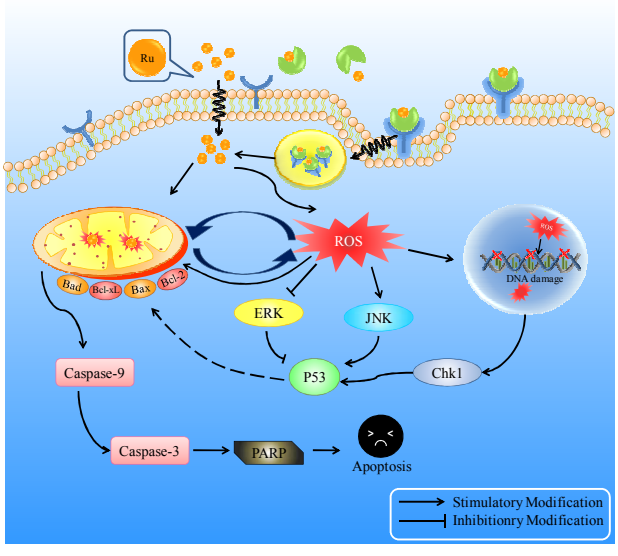

Figure 10. Proposed apoptotic signaling pathways triggered by Ru complexes in cancer cells.

Experimental Section

Materials and General Methods.

All reagents and solvents were purchased commercially and used without further purification unless specifically noted, and all aqueous solutions were prepared with doubly distilled water. 3-(4, 5-dimethylthiazol-2-yl)-2, 5-diphenyltetrazolium bromide (MTT), propidium iodide (PI), dihydroethidium (DHE), and BCA assay kit were purchased from Sigma-Aldrich.

DNA oligomers was purchased from Shanghai Sangon Biological Engineering Technology & Services (Shanghai, China) and used without further purification. The formation of intramolecular G-quadruplexes was carried out as follows: the oligomers samples, dissolved in different volume of Tris-HCl/KCl buffer (10 mM Tris-HCl, 100 mM KCl, pH 7.2) to the stock concentration of 100 μM, were heated to 90 ℃ for 5 min, gently cooled to room temperature, and then incubated at 4 ℃ overnight.

Syntheses of the ligands

The ligands pip, *p*-opip, *m*-opip, *o*-opip[30] and bbp[26] were synthesized according to a reported procedure.

Synthesis of $Ru(bbp)Cl_3$

The synthesis of $Ru(bbp)Cl_3$ was described as follows. 0.323 g (1.0 mmol) of bbp and 0.2614 g (1.0 mmol) of trihydrated ruthenium (III) chloride were dissolved in 50 mL of ethanol and refluxed for 3 h at 80 ℃. When the mixture was cooled to ambient temperature, filtered out and washed with ethanol and diethyl ether.

Synthesis of $Ru(bbp)(L)Cl(ClO_4)$

The synthesis of $Ru(bbp)(\mathbf{L})Cl(ClO_4)$. 0.1296 g (0.25 mmol) of $Ru(bbp)Cl_3$ and **L** (pip 0.074g; *p*-opip, *m*-opip or *o*-opip 0.078g) (0.25 mmol) were dissolved in 100 mL of DMF and refluxed for 5 h under a nitrogen atmosphere. The color of the solution changed from brown to reddish brown, and then the solution was cooled to ambient temperature. A red precipitate was obtained by addition of a saturated aqueous $NaClO_4$ solution, then filtered off and dried in vacuo. The products were then purified by alumina column chromatography with toluene and methanol as eluant.

$Ru(bbp)(pip)Cl(ClO_4)$(1). Yield: 35.0%, Found (%): C, 54.3; H, 2.9.0; N, 15.0. Calc. for $C_{38}H_{23}Cl_2N_9O_4Ru$ (%): C, 54.2; H, 2.8; N, 15.0. ESI-MS: m/z 742.9 (calcd mass for $C_{38}H_{23}ClN_9Ru$ $[M]^+$=742.1). Found (%): C, 54.3; H, 2.8; N, 15.1. Calc. for $C_{38}H_{23}Cl_2N_9O_4Ru$ (%): C, 54.2; H, 2.7; N, 15.0. UV-Vis (λ (nm), $\varepsilon/10^4$ (M^{-1} cm^{-1}): 299 (3.66), 684 (0.62). IR (KBr): ***ν*** 3435 (N-H), ***ν*** 1605, 1454 (C=C_{arom}) cm^{-1}. ^1H NMR (DMSO-d_6, δ ppm): 11.21 (d, 1H), 8.46-8.39 (m, 4H), 7.77-7.50 (m, 5H), 7.47 (d, 2H), 7.29-7.01 (m, 3H), 6.85 (t, 2H), 6.64 (d, 2H), 5.97 (d, 2H).

$Ru(bbp)($ *p*-opip$)Cl(ClO_4)$(2). Yield: 40.8%, Found (%):C, 53.2; H, 2.8; N, 14.6. Calc. for $C_{38}H_{23}Cl_2N_9O_5Ru$ (%): C, 53.2; H, 2.7; N, 14.7; ESI-MS: m/z 755.3 (calcd mass for $C_{38}H_{23}ClN_9ORu$ $[M]^+$=758.1), $(m/z)^{2+}$ 378.0 (calcd mass for $C_{38}H_{23}ClN_9ORu$ $[M]^{2+}$=379.1). UV-Vis (λ (nm), $\varepsilon/10^4$ ($M^{-1}cm^{-1}$):360 (2.97), 479 (0.95). IR (KBr): ***ν*** 3419 (N-H), ***ν*** 1613, 1456 (C=C_{arom}) cm^{-1}. ^1H NMR (DMSO-d_6, δ ppm): 11.18 (d, 1H), 9.88 (s, 1H), 8.52 (d, 2H), 8.38(s, 2H), 7.74 (s, 3H), 7.45 (m, 6H), 6.93 (m, 4H), 6.67 (t, 2H), 5.96 (d, 2H).

$Ru(bbp)($ *m*-opip$)Cl(ClO_4)$(3). Yield: 37.5%, Found (%):C, 53.2; H, 2.7; N, 14.6. Calc. for $C_{38}H_{23}Cl_2N_9O_5Ru$ (%): C, 53.2; H, 2.7;

N, 14.7; ESI-MS: m/*z* 782.9 (calcd mass for $C_{38}H_{23}ClN_9NaORu$ $[M+Na]^+$=781.1).UV-Vis (λ (nm), ε/10^4 (M^{-1} cm^{-1}): 287 (2.97), 492 (1.4). IR (KBr): ***ν*** 3440 (N-H), ***ν*** 1603, 1456 (C=C $_{arom}$) cm^{-1}. ^{1}H NMR (DMSO-d_6, δ ppm): 11.27 (d, 1H), 9.87 (s, 1H), 8.85 (d, 1H), 8.52 (d, 1H), 8.29 (m, 3H), 7.96 (s, 1H), 7.72 (d, 3H), 7.43 (d, 4H), 6.96 (d, 2H), 6.81 (t, 2H), 6.59 (t, 2H), 5.94 (d, 2H).

Ru(bbp)(*o*-opip)Cl(ClO_4)(4). Yield: 39.1%, Found (%):C, 53.1; H, 2.7; N, 14.5. Calc. for $C_{38}H_{23}Cl_2N_9O_5Ru$ (%): C, 53.2; H, 2.7; N, 14.7; ESI-MS: m/ *z* 755.4 (calcd mass for $C_{38}H_{23}ClN_9ORu$ $[M]^+$=758.1).UV-Vis (λ (nm), ε/10^4 (M^{-1} cm^{-1}): 280 (2.64), 336 (3.72). IR (KBr): ***ν*** 3418 (N-H), ***ν*** 1604, 1456 (C=C $_{arom}$) cm^{-1}. ^{1}H NMR (DMSO-d_6, δ ppm): 11.26 (d, 1H), 9.46 (s,1H), 9.13 (m, 2H), 8.83 (d, 2H), 8.47 (d,1H), 8.39-8.22 (m, 3H), 7,94 (dd, 2H), 7.74 (m, 3H), 7.45 (m, 2H), 6.80 (t, 2H), 6.60 (t, 2H), 5.95 (d, 2H).

Stability of Ru complexes in PBS buffer

The stability of the Ru complexes in PBS buffer was examined by UV-Vis spectrometry using a Cary 5000 UV-2450 spectrophotometer. Spectra were collected from samples dissolved in a PBS solution containing: NaCl (137 mM), KCl (2.7 mM), Na_2HPO_4 (10 mM), and KH_2PO_4 (2 mM), pH 7.4, with complexes **1**~**4** (20 μM) having 5% DMSO added to aid in solubility. Each spectrum (260 nm-750 nm) was recorded after incubation of the sample in water bath at 37 ^oC at different periods of time.

Distribution Coefficients

The distribution coefficient of each complex, defined as was experimentally determined by using the"shake-flask" method. Briefly, each complex was dissolved in a 10 mM phosphate buffer , previously saturated with octanol, to give about 1 mL of a solution with a concentration at 100 μM. The same volume of octanol (previously saturated with 10 mM phosphate buffer) was then added and the solution was shaken 100 times and equilibrated for 4.5 h.

Cell culture

The cell lines used in this study, including MCF-7 human breast adrenocarcinoma cells, Hep G2 human liver cancer cells, Hela 229 human cervical carcinoma cell, A375 human melanoma cell, HUVEC Human Umbilical Vein Endothelial Cells and HK-2 Human renal tubular epithelial cell were obtained from American Type Culture Collection (ATCC, Manassas, VA). All cell lines were maintained in DMEM media supplemented with fetal bovineserum (10%), penicillin (100 units/mL and streptomycin (50 units/mL) at 37 ℃ in CO_2 incubator (95% relative humidity, 5% CO_2).

Cell viability assay

The cell viability was determined by MTT assay which was carried out as described previously.[61]

Cellular uptake of Ru

ICP-AES method was performed to determine the cellular uptake efficiency of Ru complexes. 6×10^6 MCF-7 cells were seeded in 6 cm dishes one day before reatment and incubated at 4 °C and 37°C for 6 h with 40 μM of Ru complexes. The cells were treated with trypsin, centrifuged, washed twice in 1×PBS and Ru concentration was determined by ICP-AES method. The samples were digested with 3 mL concentrated nitric acid and 1 mL perchloric acid in an infrared rapid digestion system (Gerhardt) at 180 ℃ for 1.5 h. The digested solution was reconstituted to 10 mL with Milli-Q H_2O and used for ICP-AES analysis.

Mechanisms of cellular uptake of Ru complexes

MCF-7 cells seeded in 96-well plates at a density of 8000 cells/well and incubated in complete medium for 24 h. The cells were treated with endocytosis inhibitors for 1 h, except for nystatin (Sigma-Aldrich) that was incubated for 30 min. Treated cells were then incubated with 40 μM of Ru complex for another 6 h. The control samples were received 40 μM of Ru complexes without the addition of inhibitors. Final concentration of specific endocytosis inhibitors were listed as follows: sodium azide (NaN_3) 10 mM, 2-deoxy-Dglucose (DOG, Sigma-Aldrich) 50 mM, sucrose 0.45 M, dynasore (Sigma-Aldrich) 80 μM, nystatin 10 μg/mL. Pre-treatment of MCF-7 cells with anti-TfR antibody (1 μg/mL) was performed for 2 h at 4 ^oC, followed by the addition of **4** and further incubation for 6 h at 37 ^oC. The cells were washed with cold PBS buffer twice, followed by the lysis of cells and fluorescence intensity measurement of internalized Ru comoplexes.

Intracellular trafficking of Ru complexes

MCF-7 cells were cultured in 2 cm glass bottom dishes for 24 h. Cell lysosome, mitochondria and nuclei were stained by 50 nM of lyso-tracker DND-99 (Sigma-Aldrich) for 2 h, 50 nM Mito-Tracker Red CMXRos (Sigma-Aldrich) for 30 min and 1 μg/mL of DAPI H33258 (Sigma-Aldrich) for 30 min. After rinsed by PBS for 3 times, the cells were incubated with 40 μM of Ru complexes for various periods of time and observed by fluorescence microscopy (EVOS FL auto, Life technologies).

DNA binding experiment

DNA binding experiments were carried out in Tris-HCl/KCl buffer (10 mM Tris-HCl, 100 mM KCl, pH 7.2) using DMSO solutions of complexes **1**~**4**. The absorption titrations and fluorescence emission titrations were performed as described previously.[62] 2 μL buffered DNA solution (100 μM) was added into cuvettes in each scan. DNA binding constant (K_b) was determined by fitting the titration data to the McGhee-Von Hippel equation, as previously reported.[63, 64]

$$(\varepsilon_a-\varepsilon_f)/(\varepsilon_b-\varepsilon_f)=(b-b^2-2K_bC[DNA]/s)^{1/2}/K_bC \quad (1)$$

$$b= 1 + K_bC+ K_b[DNA]/2s \quad (2)$$

where [DNA] is the concentration of DNA, ε_a is the apparent extinction coefficient of Ru complexes at a given DNA concentration. ε_f is the extinction coefficient of Ru complexes in absence of DNA, ε_b is the extinction coefficient of Ru complexes when completely bound to DNA, C is the total Ru complex concentration, and *s* is the binding site size in base pairs. From plots of $(\varepsilon_a-\varepsilon_f)/(\varepsilon_b-\varepsilon_f)$ versus [DNA], K_b values were calculated by fitting the curves with OriginLab.

Flow cytometric analysis

The cell cycle distribution was analyzed by flow cytometry as previously described.[65] The stained cells were determined by flow cytometer (Epics-XL, Beckman Coulter) to explore cell cycle distribution, followed by data analysis using MultiCycle

software. Apoptotic cells with hypodiploid DNA contents were measured by quantifying the sub-G1 peak. For each experiment, 10000 events per sample were recorded.

Caspase Activity Assay

Caspase activities in MCF-7 cells of complexes were determined by using Caspase activity Kit (BD Biosciences) as previously described.[66] In short, the cell lysates and specific caspase substrates (include caspase-3, caspase-8 and caspase-9) were incubated at 37 ℃ for 2 h. Relative caspase activity was expressed as percentage of control (as 100%).

Western Blot Analysis

To examine the expression levels of proteins which were related to different signaling pathways with the treatment of Ru complexes, Western blot analysis was performed as in our previous studies.[37, 67]

Measurement of ROS Generation

The intracellular ROS level was examined by detecting fluorescence intensity of dihydroethidium (DHE, Beyotime) conducted by fluorescence microplate reader (excitation and emission wavelength set as 300 nm and 610 nm) as previously described.[68]

Statistics analysis

All experiments were carried out at least in triplicate and results were expressed as mean ± S.D.. Differences between two groups were analyzed by two-tailed Student's t test. Difference with $P<0.05$ (*) or $P<0.01$ (**) was considered statistically significant. The difference between three or more groups was analyzed by was analyzed by one-way ANOVA multiple comparisons.

Acknowledgements

This work was financially supported by National High Technology Research and Development Program of China (863 Program, SS2014AA020538), Science Foundation for Distinguished Young Scholars of Guangdong Province, Natural Science Foundation of China and Guangdong Province, Program for New Century Excellent Talents in University, Yang Fan Innovative & Entepreneurial Research Team Project, Research Fund for the Doctoral Program of Higher Education of China and Jinan University's Scientific Research Creativeness Cultivation Project for Outstanding Undergraduates Recommended for Postgraduate Study.

Notes and references

Department of Chemistry, Jinan University, Guangzhou 510632, China.
E-mail: tchentf@jnu.edu.cn. tzhwj@jnu.edu.cn

† Electronic Supplementary Information (ESI) available: See DOI: 10.1039/b000000x/

1. B. Rosenberg and L. Vancamp, *Nature*, 1969, **222**, 385-386.
2. G. Gasser and N. Metzler-Nolte, *Curr. Opin. Chem. Biol.*, 2012, **16**, 84-91.
3. C. S. Rajapakse, A. Martínez, B. Naoulou, A. A. Jarzecki, L. Suárez, C. Deregnaucourt, V. Sinou, J. Schrével, E. Musi and G. Ambrosini, *Inorg. Chem.*, 2009, **48**, 1122-1131.
4. A. Castonguay, C. d. Doucet, M. Juhas and D. Maysinger, *J. Med. Chem.*, 2012, **55**, 8799-8806.
5. A. Kisova, L. Zerzankova, A. Habtemariam, P. J. Sadler, V. Brabec and J. Kasparkova, *Mol. Pharm.*, 2011, **8**, 949-957.
6. G. Sava, S. Zorzet, C. Turrin, F. Vita, M. Soranzo, G. Zabucchi, M. Cocchietto, A. Bergamo, S. DiGiovine and G. Pezzoni, *Clin. Cancer. Res.*, 2003, **9**, 1898-1905.
7. C. G. Hartinger, M. A. Jakupec, S. Zorbas‐Seifried, M. Groessl, A. Egger, W. Berger, H. Zorbas, P. J. Dyson and B. K. Keppler, *Chem. Biodivers.*, 2008, **5**, 2140-2155.
8. I. Bratsos, S. Jedner, T. Gianferrara and E. Alessio, *CHIMIA*, 2007, **61**, 692-697.
9. M. R. Gill, J. Garcia-Lara, S. J. Foster, C. Smythe, G. Battaglia and J. A. Thomas, *Nat. chem.*, 2009, **1**, 662-667.
10. C. A. Puckett, R. J. Ernst and J. K. Barton, *Dalton T*, 2010, **39**, 1159-1170.
11. N. P. Cook, V. Torres, D. Jain and A. A. Martí, *J. Am. Chem. Soc.*, 2011, **133**, 11121-11123.
12. M. R. Gill and J. A. Thomas, *Chem. Soc. Rev.*, 2012, **41**, 3179-3192.
13. M. R. Gill, J. Garcia-Lara, S. J. Foster, C. Smythe, G. Battaglia and J. A. Thomas, *Nat. chem.*, 2009, **1**, 662-667.
14. L. Blackmore, R. Moriarty, C. Dolan, K. Adamson, R. J. Forster, M. Devocelle and T. E. Keyes, *Chem. Commun.*, 2013, **49**, 2658-2660.
15. H. Ke, H. Wang, W.-K. Wong, N.-K. Mak, D. W. Kwong, K.-L. Wong and H.-L. Tam, *Chem. Commun.*, 2010, **46**, 6678-6680.
16. M. J. Pisani, P. D. Fromm, Y. Mulyana, R. J. Clarke, H. Körner, K. Heimann, J. G. Collins and F. R. Keene, *ChemMedChem*, 2011, **6**, 848-858.
17. J.-F. Kou, C. Qian, J.-Q. Wang, X. Chen, L.-L. Wang, H. Chao and L.-N. Ji, *J. Biol. Inorg. Chem.*, 2012, **17**, 81-96.
18. I. Romero-Canelón, L. Salassa and P. J. Sadler, *J. Med. Chem.*, 2013, **56**, 1291-1300.
19. C. Tan, S. Lai, S. Wu, S. Hu, L. Zhou, Y. Chen, M. Wang, Y. Zhu, W. Lian and W. Peng, *J. Med. Chem.*, 2010, **53**, 7613-7624.
20. P. J. Barnard, L. E. Wedlock, M. V. Baker, S. J. Berners‐Price, D. A. Joyce, B. W. Skelton and J. H. Steer, *Angew. Chem. Int. Ed.*, 2006, **45**, 5966-5970.
21. V. Pierroz, T. Joshi, A. Leonidova, C. Mari, J. Schur, I. Ott, L. Spiccia, S. Ferrari and G. Gasser, *J. Am. Chem. Soc.*, 2012, **134**, 20376-20387.
22. D. B. Lovejoy, P. J. Jansson, U. T. Brunk, J. Wong, P. Ponka and D. R. Richardson, *Cancer Res.*, 2011, **71**, 5871-5880.
23. R. Cao, J. Jia, X. Ma, M. Zhou and H. Fei, *J. Med. Chem.*, 2013, **56**, 3636-3644.
24. T. Chen, Y. Liu, W.-J. Zheng, J. Liu and Y.-S. Wong, *Inorg. Chem.*, 2010, **49**, 6366-6368.
25. L. Li, Y.-S. Wong, T. Chen, C. Fan and W. Zheng, *Dalton T*, 2012, **41**, 1138-1141.
26. G. Li, J. Huang, M. Zhang, Y. Zhou, D. Zhang, Z. Wu, S. Wang, X. Weng, X. Zhou and G. Yang, *Chem. Commun.*, 2008, 4564-4566.
27. M. Boča, R. F. Jameson and W. Linert, *Coord. Chem. Rev.*, 2011, **255**, 290-317.
28. T. Zou, C. T. Lum, S. S. Y. Chui and C. M. Che, *Angew. Chem.*, 2013, **125**, 3002-3005.
29. W. J. Mei, J. Liu, K. C. Zheng, L. J. Lin, H. Chao, A. X. Li, F. C. Yun and L. N. Ji, *Dalton T*, 2003, 1352-1359.
30. Q. Wu, C. Fan, T. Chen, C. Liu, W. Mei, S. Chen, B. Wang, Y. Chen and W. Zheng, *Eur. J. Med. Chem.*, 2013, **63**, 57-63.
31. C. A. Puckett and J. K. Barton, *Biochemistry*, 2008, **47**, 11711-11716.
32. C. A. Puckett and J. K. Barton, *J. Am. Chem. Soc.*, 2007, **129**, 46-47.
33. L. Wang, Y. Liu, W. Li, X. Jiang, Y. Ji, X. Wu, L. Xu, Y. Qiu, K. Zhao and T. Wei, *Nano Lett.*, 2010, **11**, 772-780.
34. A. Roux, K. Uyhazi, A. Frost and P. De Camilli, *Nature*, 2006, **441**, 528-531.
35. W. Guo, W. Zheng, Q. Luo, X. C. Li, Y. Zhao, S. X. Xiong and F. Y. Wang, *Inorg. Chem.*, 2013, **52**, 5328-5338.
36. F. F. Li, M. Feterl, J. M. Warner, A. I. Day, F. R. Keene and J. G. Collins, *Dalton T*, 2013, **42**, 8868-8877.
37. Y. Huang, L. He, W. Liu, C. Fan, W. Zheng, Y.-S. Wong and T. Chen, *Biomaterials*, 2013, **34**, 7106-7116.
38. M. I. Webb, B. Wu, T. Jang, R. A. Chard, E. W. Y. Wong, M. Q. Wong, D. T. T. Yapp and C. J. Walsby, *Chem-Eur J*, 2013, **19**, 17031-

17042.
39. M. Klajner, C. Licona, L. Fetzer, P. Hebraud, G. Mellitzer, M. Pfeffer, S. Harlepp and C. Gaiddon, *Inorg. Chem.*, 2014.
40. S. J. Riedl and Y. Shi, *Nat. Rev. Mol. Cell Biol.*, 2004, **5**, 897-907.
41. M. Van Gurp, N. Festjens, G. van Loo, X. Saelens and P. Vandenabeele, *Biochem. Biophys. Res. Commun.*, 2003, **304**, 487-497.
42. L. V. Johnson, M. L. Walsh and L. B. Chen, *Proc. Natl. Acad. Sci.*, 1980, **77**, 990-994.
43. E. Liberman, V. Topaly, L. Tsofina, A. Jasaitis and V. Skulachev, *Nature*, 1969.
44. L. M. Wilhelmsson, F. Westerlund, P. Lincoln and B. Nordén, *J. Am. Chem. Soc.*, 2002, **124**, 12092-12093.
45. D. Sun and L. H. Hurley, *J. Med. Chem.*, 2009, **52**, 2863-2874.
46. J. Dash, P. S. Shirude, S.-T. D. Hsu and S. Balasubramanian, *J. Am. Chem. Soc.*, 2008, **130**, 15950-15956.
47. G. Biffi, D. Tannahill, J. McCafferty and S. Balasubramanian, *Nat. chem.*, 2013, **5**, 182-186.
48. X.-D. Wang, T.-M. Ou, Y.-J. Lu, Z. Li, Z. Xu, C. Xi, J.-H. Tan, S.-L. Huang, L.-K. An and D. Li, *J Med Chem*, 2010, **53**, 4390-4398.
49. T. Wilson, P. J. Costa, V. Félix, M. P. Williamson and J. A. Thomas, *J. Med. Chem.*, 2013, **56**, 8674-8683.
50. D. Sun, Y. Liu, D. Liu, R. Zhang, X. Yang and J. Liu, *Chem. Eur. J.*, 2012, **18**, 4285-4295.
51. G.-L. Liao, X. Chen, L.-N. Ji and H. Chao, *Chem. Commun.*, 2012, **48**, 10781-10783.
52. J. F. Turrens, *J. Physio.*, 2003, **552**, 335-344.
53. H. Pelicano, D. Carney and P. Huang, *Drug Resist. Update.*, 2004, **7**, 97-110.
54. T. Chen and Y. Wong, *Cell. Mol. Life Sci.*, 2008, **65**, 2763-2775.
55. H. Vakifahmetoglu, M. Olsson, S. Orrenius and B. Zhivotovsky, *Oncogene*, 2006, **25**, 5683-5692.
56. S. W. Lee, M. H. Lee, J. H. Park, S. H. Kang, H. M. Yoo, S. H. Ka, Y. M. Oh, Y. J. Jeon and C. H. Chung, *EMBO J.*, 2012, **31**, 4441-4452.
57. L. J. Hofseth, S. P. Hussain and C. C. Harris, *Trends Pharmacol. Sci.*, 2004, **25**, 177-181.
58. K.-R. Park, D. Nam, H.-M. Yun, S.-G. Lee, H.-J. Jang, G. Sethi, S. K. Cho and K. S. Ahn, *Cancer Lett.*, 2011, **312**, 178-188.
59. Y. Kawakami, S. E. Hartman, P. M. Holland, J. A. Cooper and T. Kawakami, *J. Immunol.*, 1998, **161**, 1795-1802.
60. G.-H. Yang, B. B. Jarvis, Y.-J. Chung and J. J. Pestka, *Toxicol. Appl. Pharmacol.*, 2000, **164**, 149-160.
61. C. Liu, Z. Liu, M. Li, X. Li, Y.-S. Wong, S.-M. Ngai, W. Zheng, Y. Zhang and T. Chen, *PLoS One*, 2013, **8**, e53945.
62. L. Li, W. Cao, W. Zheng, C. Fan and T. Chen, *Dalton T*, 2012, **41**, 12766-12772.
63. M. Carter, M. Rodriguez and A. Bard, *J. Am. Chem. Soc*, 1989, **111**, 8901-8910.
64. S. R. Dalton, S. Glazier, B. Leung, S. Win, C. Megatulski and S. J. N. Burgmayer, *J. Biol. Inorg. Chem.*, 2008, **13**, 1133-1148.
65. Y. Feng, J. Su, Z. Zhao, W. Zheng, H. Wu, Y. Zhang and T. Chen, *Dalton T*, 2014, **43**, 1854-1861.
66. Y. Zhang, X. Li, Z. Huang, W. Zheng, C. Fan and T. Chen, *Nanomed. Nanotechnol. Biol. Med.*, 2013, **9**, 74-84.
67. Y. Zhang, S. Zheng, J.-S. Zheng, K.-H. Wong, Z. Huang, S.-M. Ngai, W. Zheng, Y.-S. Wong and T. Chen, *Mol. Pharm.*, 2014.
68. C. Fan, J. Chen, Y. Wang, Y.-S. Wong, Y. Zhang, W. Zheng, W. Cao and T. Chen, *Free Radical Biol. Med.*, 2013, **65**, 305-316.

Graphical Abstract

Ruthenium complexes enter cancer cells through TfR-mediated endocytosis, and translocate to mitochondria, where they activate ROS-mediated apoptosis.